

# Globally Optimal Distributed Power Control for Nonconcave Utility Maximization

Li Ping Qian\*, Ying Jun (Angela) Zhang\*, and Mung Chiang<sup>+</sup>

\*Department of Information Engineering, The Chinese University of Hong Kong  
Shatin, New Territory, Hong Kong

<sup>+</sup>Department of Electrical Engineering, Princeton University, NJ 08544, USA  
Email: \*{lpqian6, yjzhang}@ie.cuhk.edu.hk <sup>+</sup>chiangm@princeton.edu

## Abstract

Future wireless networks are expected to operate in dense environments where the system capacity is fundamentally limited by severe co-channel interference among neighboring links. Transmit-power control has been recently explored as an important interference-mitigation technique that aims to maximize a system efficiency metric, which is often measured by a system utility function. Optimal power control is known to be difficult to achieve, mainly because the optimization problem is in general highly non-convex. This problem had eluded researchers and remained open until our recent work [11], where a centralized optimal power control algorithm, referred to as MAPEL, is developed based on a monotonic optimization framework. However, there does not yet exist a distributed power control algorithm that achieves the global optimal solution for generic utility functions, although the distributed implementation is crucial for the wireless infrastructureless networks such as ad hoc and sensor networks. This paper fills this gap by developing a distributed power control algorithm that converges to the global optimal solution for any forms of utility functions regardless of the concavity, continuity, differentiability and monotonicity. In addition, the proposed algorithm exhibits fast convergence and allows each link to update their own transmission power asynchronously.

## Index Terms

Power control, Distributed algorithm, Global optimization, Non-convex optimization.

## I. INTRODUCTION

Due to the broadcast nature of wireless medium, simultaneous transmissions on nearby links cause severe co-channel interference to each other, thus adversely affecting the performance of the system. With the increasing density of wireless devices, interference mitigation has become a critical task to alleviate the adverse effect of co-channel interference. An important interference mitigation technique is to control the transmission power of links. One commonly pursued target of transmit-power control is to maximize a system wide efficiency metric, such as a system utility function based on throughput and delay [1]-[11].

Optimal power control is known to be difficult to achieve, mainly because the optimization problem is in general non-convex due to the complicated coupling among the signal-to-interference-and-noise ratios (SINRs) of different links [10]. Finding the global optimal power allocation had eluded researchers and remained open for nearly a decade. A majority of efforts in tackling the problem is to convexify it through transformation, reparameterization, relaxation and approximation, oftentimes compromising the optimality of the solution [2], [3]. The first and probably the only global optimal power control scheme, referred to as MAPEL, that works for both concave and non-concave utility functions in all SINR regions was proposed in our recent work [11]. In contrast to other previous work that tries to tackle the non-convexity issue head on, MAPEL bypasses non-convexity by exploiting the monotonic nature of the problem. The global optimal solution thus obtained provides important benchmark and guidelines for the evaluation and design of practical heuristics targeting the same problem.

In wireless infrastructureless networks such as ad hoc and sensor networks, power control is further complicated by the lack of centralized infrastructure, which necessitates the use of distributed approaches. Distributed power control is also often preferred in infrastructure networks, since coordination across base stations in multi-cellular networks is impractical. MAPEL, however, does not serve this purpose, as the monotonic optimization framework it adopts requires centralized coordination. Existing distributed power control algorithms are likely to converge to suboptimal solutions except for few special cases. For example, the algorithms in [8], [9] obtain the unique global optimal solution only when the utility function is strictly increasing, twice differentiable, and strictly log-concave in the feasible SINR region. For the many utility functions that do not satisfy these properties, including simple utilities

such as throughput maximization, the algorithms only converge to a KKT point that is not necessarily optimal. Another thread of work is to formulate distributed power control as a noncooperative pricing game [4]-[6]. Noticeably, various assumptions are imposed on the utility functions to ensure the existence of a unique Nash equilibrium. For example, utility functions are assumed to be logarithmic in SINR [5], differentiable and quasi-concave in transmission power [4], and increasing and concave in SINR [6]. However, due to the externalities of the power control problem<sup>1</sup>, pricing-game based power control mechanisms fail to obtain the global optimal solution. An externalities-based decentralized algorithm is proposed in [7]. Therein, global optimality is obtained only when the utility function is continuous and strictly concave in transmission power, which is not the case in for most practical utility functions. To date, there does not yet exist a distributed power control algorithm that obtains the global optimal solution for general utility functions.

In this paper, we propose a distributed power control scheme that obtains the global optimal solution for any form of utility functions. The algorithm, referred to as GLAD (Gibbs samPLing based Asynchronous Distributed) algorithm, is based on the idea of Gibbs Sampling, a reinforcement learning approach. In particular, we aim to distinguish our algorithm from existing ones by the following features.

- First, the GLAD algorithm is guaranteed to converge to the global optimal power control solution regardless of the convexity, continuity, differentiability, monotonicity, and whether it is additive across links. GLAD is more widely applicable than its centralized counterpart, MAPEL, as the MAPEL algorithm requires the system utility to be monotonic in SINR.
- Second, GLAD exhibits fast convergence. In particular, our analysis shows that the algorithm converges linearly to the optimal solution.
- Third, GLAD allows asynchronous power update at each user. This is crucial to wireless infrastructureless networks due to the lack of a central clock.
- Last, for practical implementation of the algorithm, we further study how to set a “temperature” parameter of the algorithm. In particular, we provide rigorous analysis on the effect of the temperature parameter on the convergence rate and the solution quality.

<sup>1</sup> A resource allocation problem is said to have externalities if the resources allocated to each user directly affect the utility of every other user.

The rest of this paper is organized as follows. Section II introduces the system model and problem formulation. The GLAD algorithm is presented in Section III. In Section IV, we investigate the effect of temperature parameter on the system performance. The performance of GLAD is evaluated through numerical simulations in Section V. The paper is concluded in Section VI.

## II. SYSTEM FORMULATION

We consider a snapshot of wireless ad hoc network with a set of *distinct* links denoted by  $\mathcal{M} = \{1, \dots, M\}$ . Each link consists of a transmitter node  $T_i$  and a receiver node  $R_i$ . The channel gain between node  $T_i$  and node  $R_j$  is denoted by  $G_{ij}$ , which is determined by various factors such as path loss, shadowing and fading effects. We write the channel gains into a matrix form  $\mathbf{G} = [G_{ij}]$ . Let  $p_i$  denote the transmission power of link  $i$  (i.e., from node  $T_i$ ), with  $P_i^{\max}$  being its maximum allowable value. For notational convenience, we write  $\mathbf{p} = (p_i, \forall i \in \mathcal{M})$  and  $\mathbf{P}^{\max} = (P_i^{\max}, \forall i \in \mathcal{M})$  as the transmission power vector and the maximum transmission power vector, respectively. Likewise, let the noise received at  $R_i$  be  $n_i$ . Thus, the received SINR of link  $i$  is

$$\gamma_i(\mathbf{p}) = \frac{G_{ii}p_i}{\sum_{j \neq i} G_{ji}p_j + n_i}. \quad (1)$$

We aim to find the optimal power allocation  $\mathbf{p}^*$  that maximizes the overall system utility  $U(\boldsymbol{\gamma}(\mathbf{p}))$ , where  $\boldsymbol{\gamma}(\mathbf{p})$  is the vector of  $\gamma_i(\mathbf{p})$ . Mathematically, the power control problem is formulated into the following form:

$$\begin{aligned} \text{UM: } & \underset{\mathbf{p}}{\text{maximize}} && U(\boldsymbol{\gamma}(\mathbf{p})) \\ & \text{subject to} && 0 \leq p_i \leq P_i^{\max}, \forall i \in \mathcal{M}. \end{aligned} \quad (2)$$

Due to the complicated coupling of SINR across links, Problem (UM) is in general non-convex even if the objective function  $U(\cdot)$  is concave in  $\boldsymbol{\gamma}(\mathbf{p})$ , let alone the cases with non-concave  $U(\cdot)$ 's. It is worth noting that almost all previous work (e.g., [2], [3], [8], [9]) assumes that the system utility function  $U(\cdot)$  is additive across links.

That is,  $U(\boldsymbol{\gamma}(\mathbf{p})) = \sum_{i=1}^M U_i(\gamma_i(\mathbf{p}))$ , where  $U_i(\cdot)$  is the utility of link  $i$ . There are,

however, cases where the social welfare cannot be expressed as the summation of individual satisfaction.

Unlike the previous work, we do not impose any assumptions on the function  $U(\cdot)$  except for  $U(\cdot)$  being non-negative. In particular,  $U(\cdot)$  is allowed to be non-additive, discontinuous, non-differentiable, non-concave, and non-monotonic. Thus, we have full freedom to choose the utility function  $U(\cdot)$  that accurately reflects system performance. Interested readers are referred to [12] for some commonly used utility functions.

### III. THE GLAD ALGORITHM

In this section, we propose a novel algorithm, GLAD, based on Gibbs Sampling to solve Problem (UM) distributedly. For the convenience of readers, we first review some preliminaries on Gibbs Sampling in Subsection III-A before presenting the GLAD algorithm. The discrete and continuous versions of the GLAD algorithm are presented in Subsections III-B and III-C, respectively. Here, by discrete we mean transmission power can only be selected from a discrete and finite set. By continuous we mean the transmission power can be any real value between 0 and  $P_i^{\max}$ .

#### A. Mathematical Preliminaries Related to Gibbs Sampling

Gibbs Sampling was originally introduced by Gibbs in 1902 to model physical interactions between molecules and particles. Among its modern engineering applications is image processing optimization that maximizes the posterior mode estimate [13]. In particular, Gibbs Sampling solves an optimization problem with the following form

$$h^* = \min_{\mathbf{x} \in \mathcal{X}} H(\mathbf{x}), \quad (3)$$

where the variable  $\mathbf{x}$  is a  $N$ -dim row vector with element  $x_n, n=1, \dots, N$ , the feasible domain  $\mathcal{X} = \prod_{n=1}^N \mathcal{X}_n \subset \mathcal{R}^N$  (the  $N$ -dim real domain) is a compact set from the Cartesian product of the discrete sets  $\mathcal{X}_n$  corresponding to  $x_n$ , and the objective function  $H(\mathbf{x})$  can be of any form.

The key idea of Gibbs Sampling is that the value of each  $x_n$  is updated iteratively and asynchronously according to a probability distribution, which by itself is also

adjusted at each iteration according to the observations of  $x_1, \dots, x_{n-1}, x_{n+1}, \dots, x_N$ . Presumably, the value of  $x_n$  that yields a smaller  $H(\mathbf{x})$  is more likely to be picked. The details of Gibbs Sampling is given in Algorithm 1.

According to (4), an  $x_n$  that yields a better objective function value (i.e., a smaller  $H(\cdot)$  here) will be picked with a higher probability. This is especially true when  $\beta$  is large. In fact, as we will prove in the next subsection, the power control algorithm based on Gibbs Sampling can converge to the global optimal solution when  $\beta$  approaches infinity.

---

**Algorithm 1** Gibbs Sampling [14]

---

1: **Initialization:** Randomly select an initial point  $\mathbf{x} \in \mathcal{X}$ .

2: **loop**

3:   **for all**  $n$ 's in any order **do**

4:     The element  $x_n$  is updated by a sample from the probability distribution

$$\Lambda_n(\mathbf{x}_{-n}) = (\Lambda_n(x_n | \mathbf{x}_{-n}), \forall x_n \in \mathcal{X}_n) \text{ with}$$

$$\Lambda_n(x_n | \mathbf{x}_{-n}) = \frac{\exp(-\beta H(x_n, \mathbf{x}_{-n}))}{\sum_{x_n \in \mathcal{X}_n} \exp(-\beta H(x_n, \mathbf{x}_{-n}))}, \quad (4)$$

where  $\beta$  is a positive constant, and  $\mathbf{x}_{-n} = (x_1, \dots, x_{n-1}, x_{n+1}, \dots, x_N)$ .

5:   **end for**

6: **end loop**

---

### B. Discrete-GLAD

Assuming that each  $p_i$  can only take values from a discrete set  $\mathcal{P}_i^D = \{0, \Delta P_i, 2\Delta P_i, \dots, P_i^{\max}\}$ , Gibbs Sampling can be straightforwardly applied to solve Problem (UM). In what follows, we present the Discrete-GLAD algorithm and prove its convergence to the set of global optimal solutions.

#### 1) Algorithm Description

Based on the idea of Gibbs-Sampling, Discrete-GLAD works as follows. Each link  $i$  picks a sequence of time epochs  $\{t_{i1}, t_{i2}, \dots\}$ , at which its transmission power is updated. In particular, at the time epoch  $t_{ik}$ , the transmission power is updated to  $p_i(t_{ik})$  according to the probability distribution

$\mathcal{A}_i(\mathbf{p}_{-i}(t_{ik}-)) = (\Lambda_i(p_i | \mathbf{p}_{-i}(t_{ik}-)), \forall p_i \in \mathcal{P}_i^D)$ , i.e.,

$$\Lambda_i(p_i | \mathbf{p}_{-i}(t_{ik}-)) = \frac{\exp(\frac{-\beta}{U(\boldsymbol{\gamma}(p_i, \mathbf{p}_{-i}(t_{ik}-)))})}{\sum_{p_i \in \mathcal{P}_i^D} \exp(\frac{-\beta}{U(\boldsymbol{\gamma}(p_i, \mathbf{p}_{-i}(t_{ik}-)))})}, \quad (5)$$

where  $\mathbf{p}_{-i}(t_{ik}-) = (p_1(t_{ik}-), \dots, p_{i-1}(t_{ik}-), p_{i+1}(t_{ik}-), \dots, p_M(t_{ik}-))$  is the transmission power of all other links except link  $i$  before the time instant  $t_{ik}$ . Likewise,  $\boldsymbol{\gamma}(p_i, \mathbf{p}_{-i}(t_{ik}-))$  is the vector of  $\gamma_i(p_i, \mathbf{p}_{-i}(t_{ik}-))$ , which is the SINR of link  $i$  under transmission power vector  $(p_i, \mathbf{p}_{-i}(t_{ik}-))$ . In particular, the vectors  $\boldsymbol{\gamma}(p_i, \mathbf{p}_{-i}(t_{ik}-))$  and  $\boldsymbol{\gamma}(p_i', \mathbf{p}_{-i}(t_{ik}-))$  in (5) can be calculated at the transmitter side of link  $i$  as follows

$$\boldsymbol{\gamma}_j(p_i, \mathbf{p}_{-i}(t_{ik}-)) = \begin{cases} \frac{\gamma_j(\mathbf{p}(t_{ik}-))p_i}{p_i(t_{ik}-)}, & j = i \\ \frac{s_j(t_{ik}-)}{\frac{s_j(t_{ik}-)}{\gamma_j(\mathbf{p}(t_{ik}-))} + G_{ij}(p_i - p_i(t_{ik}-))}, & j \neq i, \end{cases}$$

$$\boldsymbol{\gamma}_j(p_i', \mathbf{p}_{-i}(t_{ik}-)) = \begin{cases} \frac{\gamma_j(\mathbf{p}(t_{ik}-))p_i'}{p_i(t_{ik}-)}, & j = i \\ \frac{s_j(t_{ik}-)}{\frac{s_j(t_{ik}-)}{\gamma_j(\mathbf{p}(t_{ik}-))} + G_{ij}(p_i' - p_i(t_{ik}-))}, & j \neq i, \end{cases} \quad (6)$$

where  $s_j(t_{ik}-) = G_{jj}p_j(t_{ik}-)$  is the received signal power of link  $j$  just before the time instant  $t_{ik}$ . Suppose that each link knows the system utility function  $U(\cdot)$  and has the memory of transmission power used before the time instant  $t_{ik}$  (i.e.,  $p_i(t_{ik}-)$ ). As is common in cellular networks, assume that the transmitter  $T_i$  has the knowledge of  $G_{ij}$  by measuring the received power of the control packets sent by the receiver  $R_j$ . This can be achieved by the reciprocity of the channel. Then, in order to calculate  $\mathcal{A}_i(\mathbf{p}_{-i}(t_{ik}-))$ , all that link  $i$  needs from other links are  $\boldsymbol{\gamma}_j(\mathbf{p}(t_{ik}-))$ 's and  $s_j(t_{ik}-)$ 's. These two values can be measured at the receiver side of link and broadcasted to other links in a control packet every time the receiver of link  $j$  senses a change in its received SINR or received power. Note that the convergence of Discrete-GLAD would still be guaranteed even if the information about  $\boldsymbol{\gamma}_j(\mathbf{p}(t_{ik}-))$ 's and  $s_j(t_{ik}-)$ 's is not updated in time. This will be discussed in our future work.

Having introduced the basic operations, we now present the Discrete-GLAD algorithm in Algorithm 2.

---

**Algorithm 2** The Discrete-SEER Algorithm

---

**The implementation at each transmitter node  $T_i$**

- 1: **Initialization:** pick a sequence of time epochs  $\{t_{i1}, t_{i2}, \dots\}$  in continuous time.
- 2: Choose some feasible power  $p_i(t_{i1}) \in \mathcal{P}_i^D$ . Let  $k = 1$ .
- 3: **repeat**
- 4: Transmit the data packet with the power level  $p_i(t_{ik})$ .
- 5: Keep sensing the control packets broadcasted by receivers, and then update the information of  $\gamma_j$ 's and  $s_j$ 's.
- 6:  $k = k + 1$ .
- 7: Update the feasible power  $p_i(t_{ik}) \in \mathcal{P}_i^D$  according to the probability distribution given in (5).
- 8: **until** Link  $i$  decides to leave the network

**The implementation at each receiver node  $R_i$**

- 1: **repeat**
  - 2: Keep measuring its received SINR and received power, and broadcast them in a control packet when a change in the SINR or power is sensed.
  - 3: **until** Link  $i$  leaves the network
- 

## 2) Global Convergence

In this subsection, we investigate the convergence of Discrete-GLAD. The following Theorem 1 shows that given  $\beta$ , Discrete-GLAD converges to a strategy that picks feasible solutions to Problem (UM) with a unique stationary distribution. Especially, as  $\beta$  becomes very large, the strategy corresponds to the one that picks global optimal solutions to Problem (UM) with probability 1. When there are multiple global optimal solutions, one is picked uniformly among them.

**Theorem 1.** *Starting from any initial power allocation, Discrete-GLAD corresponds to a Markov chain that converges to a stationary distribution*

$\Omega_\beta = (\Omega_\beta(\mathbf{p}), \forall \mathbf{p} \in \mathcal{P}^D)$ , i.e.,

$$\Omega_\beta(\mathbf{p}) = \frac{\exp(\frac{-\beta}{U(\gamma(\mathbf{p}))})}{\sum_{\mathbf{p}' \in \mathcal{P}^D} \exp(\frac{-\beta}{U(\gamma(\mathbf{p}'))})}, \quad (7)$$

where  $\mathcal{P}^D = \{\mathbf{p} \mid p_i \in \mathcal{P}_i^D, \forall i\}$ . When  $\beta \rightarrow \infty$ ,  $\Omega_\beta(\mathbf{p})$  becomes

$$\lim_{\beta \rightarrow \infty} \Omega_\beta(\mathbf{p}) = \Omega_\infty(\mathbf{p}) = \begin{cases} \frac{1}{|\mathcal{P}^{D^*}|} & \text{if } \mathbf{p} \in \mathcal{P}^{D^*}, \\ 0 & \text{otherwise,} \end{cases} \quad (8)$$

where  $\mathcal{P}^{D^*}$  is the set of global optimal solutions to Problem (UM) with discrete power allocation, and  $|\mathcal{P}^{D^*}|$  denotes the cardinality of  $\mathcal{P}^{D^*}$ .

*Proof:* A close look at the Discrete-GLAD algorithm shows that a transition from one transmission power vector  $\mathbf{p}_1$  to another  $\mathbf{p}_2$  occurs only when some link, say link  $i$ , updates its transmission power according to its observation on the other entries of  $\mathbf{p}_1$ . In other words, the transition does not depend on the power vectors before  $\mathbf{p}_1$ . Hence, Discrete-GLAD can be modeled as a Markov chain whose transition matrix corresponding to link  $i$ 's update is defined as  $\mathbf{\Pi}_i = [\Pi_i(\mathbf{p}_1, \mathbf{p}_2), \forall \mathbf{p}_1, \mathbf{p}_2 \in \mathcal{P}^D]$ , where

$$\Pi_i(\mathbf{p}_1, \mathbf{p}_2) = \begin{cases} \Lambda_i(p_{2,i} | \mathbf{p}_{1,-i}) & \text{if } \mathbf{p}_{1,-i} = \mathbf{p}_{2,-i} \\ 0 & \text{otherwise.} \end{cases} \quad (9)$$

Here,  $\mathbf{p}_{1,-i} = (p_{1,1}, \dots, p_{1,i-1}, p_{1,i+1}, \dots, p_{1,M})$  is the transmission power vector of link  $i$ 's opponents, and  $\mathbf{p}_{2,-i}$  is defined likewise. Generally, each link schedules their power updates at arbitrary time epochs in continuous time. Therefore, there are no simultaneous updates with probability 1. The resulting Markov chain is actually a composition of single-link transition probabilities.

To prove the former part of Theorem 1, we just need to prove that for any updating order, the Markov chain specified in (9) has a stationary distribution. A close look at

(9) reveals the fact that  $\prod_{i=1}^M \mathbf{\Pi}_i$  is strictly positive, which implies that the Markov chain is ergodic. Therefore, its stationary distribution exists. Given an arbitrary updating order  $\{i_1, i_2, i_3, \dots\}$ , the distribution  $\Omega_\beta$  given in (7) always satisfies

$$\Omega_\beta \cdot \mathbf{\Pi}_{i_1} \cdot \mathbf{\Pi}_{i_2} \cdot \mathbf{\Pi}_{i_3} \cdots = \underbrace{\Omega_\beta \cdot \mathbf{\Pi}_{i_1}}_{\Omega_\beta} \cdot \mathbf{\Pi}_{i_2} \cdot \mathbf{\Pi}_{i_3} \cdots = \underbrace{\underbrace{\Omega_\beta \cdot \mathbf{\Pi}_{i_1} \cdot \mathbf{\Pi}_{i_2}}_{\Omega_\beta}}_{\Omega_\beta} \cdot \mathbf{\Pi}_{i_3} \cdots = \Omega_\beta. \quad (10)$$

Consequently,  $\Omega_\beta$  is the stationary distribution of the Markov chain (i.e., the stationary distribution of Discrete-GLAD) for any updating order.

Now, we prove the latter part of Theorem 1. Let  $U^* = \max_{\mathbf{p} \in \mathcal{P}^D} U(\gamma(\mathbf{p}))$  and

$\Delta \frac{1}{U(\mathbf{p})} = \frac{1}{U(\boldsymbol{\gamma}(\mathbf{p}))} - \frac{1}{U^*}$ . Then,

$$\begin{aligned} \Omega_\beta(\mathbf{p}) &= \frac{\exp(\frac{-\beta}{U(\boldsymbol{\gamma}(\mathbf{p}))})}{\sum_{\mathbf{p} \in \mathcal{P}^D} \exp(\frac{-\beta}{U(\boldsymbol{\gamma}(\mathbf{p}))})} = \frac{\exp(-\beta \Delta \frac{1}{U(\mathbf{p})})}{|\mathcal{P}^{D^*}| + \sum_{\mathbf{p}': U(\boldsymbol{\gamma}(\mathbf{p}')) < U^*} \exp(-\beta \Delta \frac{1}{U(\mathbf{p}')})} \\ &\xrightarrow{\beta \rightarrow \infty} \Omega_\infty(\mathbf{p}) = \begin{cases} \frac{1}{|\mathcal{P}^{D^*}|} & \text{if } \mathbf{p} \in \mathcal{P}^{D^*} \\ 0 & \text{otherwise} \end{cases} \end{aligned} \quad (11)$$

Consequently, the latter part of Theorem 1 follows.  $\blacksquare$

### C. Continuous-GLAD

#### 1) Algorithm Description

In the last subsection, we have assumed that  $p_i$  can only take values from a finite and discrete set. However, the original Problem (UM) allows  $p_i$  to be any real number in  $[0, P_i^{\max}]$ . One straightforward way to extend Discrete-GLAD to the continuous power allocation case is to let  $\Delta P_i$  be very small (close to 0). However, a direct consequence is that each link now needs an excessively large memory space to store the probability distribution vector  $\Lambda_i(\mathbf{p}_{-i}(t_{ik}-))$ . To solve this issue, we have the following observation when  $\Delta P_i \rightarrow 0$ .

$$\begin{aligned} \Lambda_i(p_i | \mathbf{p}_{-i}(t_{ik}-)) &= \lim_{\Delta P_i \rightarrow 0} \frac{\exp(\frac{-\beta}{U(\boldsymbol{\gamma}(p_i, \mathbf{p}_{-i}(t_{ik}-)))}) \Delta P_i}{\Delta P_i \sum_{p_i \in \mathcal{P}_i^D} \exp(\frac{-\beta}{U(\boldsymbol{\gamma}(p_i, \mathbf{p}_{-i}(t_{ik}-)))})} \\ &= \lim_{\Delta P_i \rightarrow 0} \frac{\exp(\frac{-\beta}{U(\boldsymbol{\gamma}(p_i, \mathbf{p}_{-i}(t_{ik}-)))}) \Delta P_i}{\int_0^{P_i^{\max}} \exp(\frac{-\beta}{U(\boldsymbol{\gamma}(p_i, \mathbf{p}_{-i}(t_{ik}-)))}) dp_i'} \end{aligned} \quad (12)$$

This can be transformed into a probability density function (pdf)

$$f_i(p_i | \mathbf{p}_{-i}(t_{ik}-)) = \lim_{\Delta P_i \rightarrow 0} \frac{\Lambda_i(p_i, \mathbf{p}_{-i}(t_{ik}-))}{\Delta P_i} = \frac{\exp(\frac{-\beta}{U(\boldsymbol{\gamma}(p_i, \mathbf{p}_{-i}(t_{ik}-)))})}{\int_0^{P_i^{\max}} \exp(\frac{-\beta}{U(\boldsymbol{\gamma}(p_i, \mathbf{p}_{-i}(t_{ik}-)))}) dp_i'}, \forall p_i \in \mathcal{P}_i^C \quad (13)$$

where  $\mathcal{P}_i^C = \{p_i | 0 \leq p_i \leq P_i^{\max}\}$ . With this, Continuous-GLAD works as follows. Each link  $i$  updates its feasible transmission power  $p_i \in \mathcal{P}_i^C$  at each time instant  $t_{ik}$  with the pdf (13). By doing so, we avoid the need for a large memory space to store  $\Lambda_i(\mathbf{p}_{-i}(t_{ik}-))$ . Note that in (13), the vectors  $\boldsymbol{\gamma}(p_i, \mathbf{p}_{-i}(t_{ik}-))$  and  $\boldsymbol{\gamma}(p_i', \mathbf{p}_{-i}(t_{ik}-))$  can be calculated in the same way as (6). Thus, the algorithm of Continuous-GLAD is the same as Discrete-GLAD except for Step 7, which is

modified as follows.

---

*Step 7.* Choose a feasible power  $p_i(t_{ik}) \in \mathcal{P}_i^{C^*}$  according to the pdf given in (13).

---

## 2) Global Convergence

The following Theorem shows that the optimal solution to Problem (UM) can be achieved through Continuous-GLAD with large  $\beta$ .

**Theorem 2.** *Starting from any initial power allocation, Continuous-GLAD corresponds to a Markov chain that converges to a stationary joint pdf*

$$f_\beta(\mathbf{p}) = \frac{\exp(\frac{-\beta}{U(\mathbf{p})})}{\int_0^{\mathbf{p}^{\max}} \exp(\frac{-\beta}{U(\mathbf{p}')} ) d\mathbf{p}'}, \forall \mathbf{p} \in \mathcal{P}^C \quad (14)$$

where  $\mathcal{P}^C = \{\mathbf{p} | 0 \leq p_i \leq P_i^{\max}, \forall i \in M\}$ . When  $\beta \rightarrow \infty$ ,  $f_\beta(\mathbf{p})$  becomes

$$\lim_{\beta \rightarrow \infty} f_\beta(\mathbf{p}) = f_\infty(\mathbf{p}) = \frac{1}{|\mathcal{P}^{C^*}|} \delta_{\mathbf{p}}(\mathcal{P}^{C^*}), \quad (15)$$

where the function  $\delta_{\mathbf{p}}(\mathcal{P}^{C^*})$  satisfies

$$\delta_{\mathbf{p}}(\mathcal{P}^{C^*}) = \begin{cases} +\infty, & \text{if } \mathbf{p} \in \mathcal{P}^{C^*} \\ 0, & \text{otherwise} \end{cases}$$

and  $\int_0^{\mathbf{p}^{\max}} \delta_{\mathbf{p}}(\mathcal{P}^{C^*}) d\mathbf{p} = |\mathcal{P}^{C^*}|$ . Here,  $\mathcal{P}^{C^*}$  is the set of global optimal solutions of Problem (UM) and  $|\mathcal{P}^{C^*}|$  denotes its cardinality. In other words, Continuous-GLAD converges to a strategy that selects global optimal power allocation with probability 1.

The proof of Theorem 2 is similar to that of Theorem 1, and thus omitted due to space limitation.

## IV. EFFECT OF THE TEMPERATURE PARAMETER $\beta$

Theorem 1 and 2 indicate that the global optimal solution is obtained when  $\beta$  is set to be very large. In real implementation of the algorithm, however, there are more practical concerns regarding the selection of  $\beta$ . In (5) and (13),  $\beta$  reflects the degree of greediness. A very small  $\beta$  causes all possible values of  $p_i$  to be chosen (nearly) equiprobably. Setting  $\beta$  to be small may result in poor solution quality, as the algorithm will converge to a point where non-optimal solutions are picked with non-negligible probability. On the contrary, when  $\beta \rightarrow \infty$ , the algorithm becomes a

greedy one that only picks the  $p_i$ 's that maximize  $U(\cdot)$  for given  $p_{-i}$ . At the early stages of the algorithm run, setting  $\beta$  to be too large may cause the algorithm to be stuck in a local optimum for a long time before exploring other less greedy power allocations. It is thus obvious that  $\beta$  affects not only the optimality of the solution but also the convergence rate. There have been studies on dynamically adjusting  $\beta$  during the run of the algorithm to ensure fast convergence rate and good solution quality [13], [15]. This, however, requires coordination across the network, and hence is not preferred in distributed power control. In the following, we analyze the effect of  $\beta$  on the performance of the algorithm. The results will serve as a useful guideline for choosing appropriate  $\beta$  in the GLAD algorithm.

#### A. The Rate of Convergence

Theorems 1 and 2 establish the convergence of GLAD, but not the rate of convergence. The convergence rate of Gibbs Sampling based algorithms is generally difficult to obtain [16]. In what follows, we simplify the problem by assuming that links update their transmission power in an arbitrary but fixed updating order  $\{i_1, i_2, i_3, \dots\}$ , say for example  $\{1, 2, \dots, M\}$  with repetition. In particular, we say one round of update is done when all links have updated their transmission power once according to the updating order. In the following, we use round and iteration interchangeably.

For simplicity, we first investigate the convergence rate of Discrete-GLAD. One way to measure the convergence rate is to observe the total variation distance [17], defined as follows, between two probability distributions  $\Omega_\beta^{(k)} = (\Omega_\beta^{(k)}(\mathbf{p}), \forall \mathbf{p} \in \mathcal{P}^D)$  and  $\Omega_\beta$ , where  $\Omega_\beta^{(k)}$  is the probability distribution on the feasible power set  $\mathcal{P}^D$  after the  $k$ th round of power update.

**Definition 1.** The total variation distance between two probability distributions  $\Omega_\beta^{(k)}$  and  $\Omega_\beta$  is defined as

$$\|\Omega_\beta^{(k)} - \Omega_\beta\|_{\text{var}} = \frac{1}{2} \sum_{\mathbf{p} \in \mathcal{P}^D} |\Omega_\beta^{(k)}(\mathbf{p}) - \Omega_\beta(\mathbf{p})|. \quad (17)$$

**Theorem 3.** *Discrete-GLAD converges linearly to the stationary distribution  $\Omega_\beta$  in total variation distance. That is,*

$$\|\mathbf{\Omega}_\beta^{(k)} - \mathbf{\Omega}_\beta\|_{\text{var}} \leq c_\beta |\lambda_{2\beta}|^k, \quad (18)$$

where  $c_\beta$  is a positive constant with respect to matrix  $\prod_{i=1}^M \mathbf{\Pi}_i$ , and  $\lambda_{2\beta}$  is the second largest eigenvalue of matrix  $\prod_{i=1}^M \mathbf{\Pi}_i$  satisfying  $0 < |\lambda_{2\beta}| < 1$  in magnitude.

The proof is relegated to Appendix A.

According to Theorem 3, the following Corollary is straightforward.

**Corollary 1.** For any  $\varepsilon > 0$ , Discrete-GLAD guarantees that the total variation distance between  $\mathbf{\Omega}_\beta^{(k)}$  and  $\mathbf{\Omega}_\beta$  is smaller than  $\varepsilon$  after  $\left\lceil \frac{\log \varepsilon - \log c_\beta}{\log |\lambda_{2\beta}|} \right\rceil$  iterations<sup>2</sup>. That is, the iteration complexity of Discrete-GLAD is  $O\left(\frac{\log \varepsilon}{\log |\lambda_{2\beta}|}\right)$ .

The statements in Theorem 3 and Corollary 1 can be extended to Continuous-GLAD, as Continuous-GLAD is essentially an extreme case of Discrete-GLAD when  $\Delta P_i \rightarrow 0$  for all  $i$ . Let  $f_\beta^{(k)}(\mathbf{p})$  denote the joint pdf on the feasible transmission power set  $\mathcal{P}^C$  when the  $k$ th iteration is completed, and let  $\mathbf{\Pi}'_i$  denote  $\lim_{\Delta P_i \rightarrow 0} \mathbf{\Pi}_i$ . Then, the convergence rate of Continuous-GLAD is given in the following Theorem 4.

**Theorem 4.** *Continuous-GLAD converges linearly to the stationary joint pdf  $f_\beta(\mathbf{p})$  in total variation distance. That is,*

$$\int_{\mathbf{0}}^{\mathbf{p}^{\max}} |f_\beta^{(k)}(\mathbf{p}) - f_\beta(\mathbf{p})| d\mathbf{p} \leq c'_\beta |\lambda'_{2\beta}|^k, \quad (19)$$

where  $c'_\beta$  is a positive constant with respect to matrix  $\prod_{i=1}^M \mathbf{\Pi}'_i$ , and  $\lambda'_{2\beta}$  is the second largest eigenvalue of matrix  $\prod_{i=1}^M \mathbf{\Pi}'_i$  satisfying  $0 < |\lambda'_{2\beta}| < 1$  in magnitude.

The proof of Theorem 4 is similar to that of Theorem 3, and thus omitted due to space limitation.

It is clear that the second largest eigenvalue  $\lambda_{2\beta}$  of matrix  $\prod_{i=1}^M \mathbf{\Pi}_i$  (or  $\lambda'_{2\beta}$  of matrix  $\prod_{i=1}^M \mathbf{\Pi}'_i$ ) is associated with  $\beta$ . In particular, Fig. 1 shows that the second

<sup>2</sup> $\lceil x \rceil$  denotes the smallest integer that is larger than or equal to  $x$ .

largest eigenvalue  $\lambda_{2\beta}$  follows a decreasing trend and approaches 0 when  $\beta$  is very large. Thus, different  $\beta$  leads to different convergence rate. This will be further illustrated through numerical simulations in Section V.

### B. The Optimality of the Solution

In this subsection, we investigate the effect of  $\beta$  on the optimality of the solution. Specifically, we discuss some characteristic features of GLAD when the algorithm converges, i.e., at the stationary distribution  $\Omega_\beta$  (or the stationary joint pdf  $f_\beta(\mathbf{p})$ ). First of all, we observe in Theorem 5 the dependence of the stationary distribution  $\Omega_\beta$  (or the stationary joint pdf  $f_\beta(\mathbf{p})$ ) on  $\beta$ .

**Theorem 5.** *The probability of converging to a global optimal solution to Problem (UM) monotonically increases with the increase of  $\beta$ .*

*Proof:* We focus on Discrete-GLAD in this proof. The proof for Continuous-GLAD is similar and hence omitted.

To prove Theorem 5, we calculate the following derivative from (7)

$$\frac{\partial \Omega_\beta(\mathbf{p})}{\partial \beta} = \frac{\partial}{\partial \beta} \frac{\exp(\frac{-\beta}{U(\mathbf{y}(\mathbf{p}))})}{\sum_{\mathbf{p} \in \mathcal{P}^D} \exp(\frac{-\beta}{U(\mathbf{y}(\mathbf{p}))})} = \Omega_\beta(\mathbf{p}) \left( \langle U^{-1} \rangle_\beta - \frac{1}{U(\mathbf{y}(\mathbf{p}))} \right), \quad (20)$$

where  $\langle U^{-1} \rangle_\beta$  denotes the expected inverse system utility over  $\Omega_\beta$ , i.e.,

$$\langle U^{-1} \rangle_\beta = \sum_{\mathbf{p} \in \mathcal{P}^D} \frac{\Omega_\beta(\mathbf{p})}{U(\mathbf{y}(\mathbf{p}))}. \quad (21)$$

The sign of  $\frac{\partial \Omega_\beta(\mathbf{p})}{\partial \beta}$  is determined by the sign of  $\langle U^{-1} \rangle_\beta - \frac{1}{U(\mathbf{y}(\mathbf{p}))}$  as  $\Omega_\beta(\mathbf{p}) > 0$  for all  $\mathbf{p} \in \mathcal{P}^D$ . Note that  $\frac{1}{U(\mathbf{y}(\mathbf{p}))} < \langle U^{-1} \rangle_\beta$  if  $\mathbf{p} \in \mathcal{P}^{D*}$ . Consequently,  $\frac{\partial \Omega_\beta(\mathbf{p})}{\partial \beta} > 0$  for every optimal solution  $\mathbf{p} \in \mathcal{P}^{D*}$ , implying that  $\Omega_\beta(\mathbf{p})$  for  $\mathbf{p} \in \mathcal{P}^{D*}$  monotonically increases with  $\beta$ . ■

The fact that GLAD converges to a probability distribution  $\Omega_\beta$  (or  $f_\beta(\mathbf{p})$ ) implies that the system utility obtained at convergence is itself a random variable. Such random variable becomes deterministic and equal to the maximum achievable system utility when  $\beta \rightarrow \infty$ . Theorem 6 and 7 investigate the effect of  $\beta$  on the mean and variance of the obtained utility.

**Theorem 6.** When the algorithm converges, the expected value of obtained utility, denoted by  $\bar{U}_\beta = \sum_{\mathbf{p} \in \mathcal{P}^D} \Omega_\beta(\mathbf{p})U(\gamma(\mathbf{p}))$  for Discrete-GLAD (or

$\bar{U}_\beta = \int_0^{\mathbf{p}^{\max}} U(\gamma(\mathbf{p}))f_\beta(\mathbf{p})d\mathbf{p}$  for Continuous-GLAD), monotonically increases with the increase of  $\beta$ . Especially,  $\bar{U}_\infty$  is equal to  $U^*$  when  $\beta \rightarrow \infty$ .

*Proof:* We mainly focus on Discrete-GLAD for the proof. The proof for Continuous-GLAD is similar, and hence omitted. Taking the derivative of  $\bar{U}_\beta$ , we get

$$\begin{aligned} \frac{\partial \bar{U}_\beta}{\partial \beta} &= \sum_{\mathbf{p} \in \mathcal{P}^D} \Omega_\beta(\mathbf{p})U(\gamma(\mathbf{p})) \left( \langle U^{-1} \rangle_\beta - \frac{1}{U(\gamma(\mathbf{p}))} \right) \\ &= \sum_{\mathbf{p} \in \mathcal{P}^D} \Omega_\beta(\mathbf{p})U(\gamma(\mathbf{p})) \sum_{\mathbf{p}' \in \mathcal{P}^D} \frac{\Omega_\beta(\mathbf{p}')}{U(\gamma(\mathbf{p}'))} - 1 \\ &> \sum_{\mathbf{p} \in \mathcal{P}^D} \left( \Omega_\beta(\mathbf{p})U(\gamma(\mathbf{p})) \right)^{\frac{1}{2}} \left( \frac{\Omega_\beta(\mathbf{p})}{U(\gamma(\mathbf{p}))} \right)^{\frac{1}{2}} - 1 \\ &= \sum_{\mathbf{p} \in \mathcal{P}^D} \Omega_\beta(\mathbf{p}) - 1 = 1 - 1 = 0, \end{aligned} \quad (22)$$

where the inequality is due to the Holder's inequality. This implies the mean  $\bar{U}_\beta$  monotonically increases with the increase of  $\beta$ . When  $\beta \rightarrow \infty$ ,  $\Omega_\infty(\mathbf{p})$  is equal to  $\frac{1}{|\mathcal{P}^{D^*}|}$  for  $\mathbf{p} \in \mathcal{P}^{D^*}$ , and equal to zero otherwise. Thus  $\bar{U}_\infty = \sum_{\mathbf{p} \in \mathcal{P}^{D^*}} \frac{1}{|\mathcal{P}^{D^*}|} U(\gamma(\mathbf{p})) = U^*$ . ■

**Theorem 7.** For any  $\delta \geq 0$ , there exists a  $\beta(\delta)$  such that the variance of the obtained utility at convergence, denoted by  $V_\beta(U) = \sum_{\mathbf{p} \in \mathcal{P}^D} (U(\gamma(\mathbf{p})) - \bar{U}_\beta)^2 \Omega_\beta(\mathbf{p})$  for

Discrete-GLAD (or  $V_\beta(U) = \int_0^{\mathbf{p}^{\max}} (U(\gamma(\mathbf{p})) - \bar{U}_\beta)^2 f_\beta(\mathbf{p})d\mathbf{p}$  for Continuous-GLAD), is smaller than  $\delta$  for all  $\beta \geq \beta(\delta)$ . In particular,  $\beta(\delta)$  is given by

$$\begin{cases} \beta(\delta) = 0, & \text{if } \delta \geq U^{*2} \left(1 + \frac{|\mathcal{P}^{D^*}|}{|\mathcal{P}^D|}\right)^2 + (U^* - U_*)^2 \left(1 + \frac{|\mathcal{P}^{D^*}|}{|\mathcal{P}^D|}\right), \\ \Omega_{\beta(\delta)}(\mathbf{p}) = \frac{1 + \frac{(U^* - U_*)^2}{2U^{*2}} - \sqrt{\frac{\delta}{U^{*2}} + \frac{(U^* - U_*)^4}{4U^{*4}}}}{|\mathcal{P}^{D^*}|}, & \forall \mathbf{p} \in \mathcal{P}^{D^*}, \text{ otherwise} \end{cases} \quad (23)$$

for Discrete-GLAD, where  $U_* = \min_{\mathbf{p} \in \mathcal{P}^D} U(\gamma(\mathbf{p}))$ , and

$$\begin{cases} \beta(\delta) = 0, & \text{if } \delta \geq U^{*2} \left(1 + \frac{\int_{p \in \mathcal{P}^{C^*}} dp}{\int_{p \in \mathcal{P}^C} dp}\right)^2 + (U^* - U_*)^2 \left(1 + \frac{\int_{p \in \mathcal{P}^{C^*}} dp}{\int_{p \in \mathcal{P}^C} dp}\right), \\ \Omega_{\beta(\delta)}(\mathbf{p}) = \frac{1 + \frac{(U^* - U_*)^2}{2U^{*2}} \sqrt{\frac{\delta}{U^{*2}} + \frac{(U^* - U_*)^4}{4U^{*4}}}}{\int_{p \in \mathcal{P}^{C^*}} dp}, & \forall \mathbf{p} \in \mathcal{P}^{D^*}, \text{ otherwise} \end{cases} \quad (24)$$

for Continuous-GLAD, where  $U_* = \min_{p \in \mathcal{P}^C} U(\gamma(\mathbf{p}))$ .

*Proof:* Like before, we focus on Discrete-GLAD for the proof. The proof for Continuous-GLAD is similar. Note that

$$\begin{aligned} \bar{U}_\beta &= \sum_{\mathbf{p}' \in \mathcal{P}^{D^*}} U(\gamma(\mathbf{p}')) \Omega_\beta(\mathbf{p}') + \sum_{\mathbf{p}' \notin \mathcal{P}^{D^*}} U(\gamma(\mathbf{p}')) \Omega_\beta(\mathbf{p}') \\ &\geq \sum_{\mathbf{p}' \in \mathcal{P}^{D^*}} U(\gamma(\mathbf{p}')) \Omega_\beta(\mathbf{p}') \end{aligned} \quad (25)$$

due to the fact that  $U(\cdot)$  is non-negative for any feasible power allocation. Since  $\Omega_\beta(\mathbf{p}')$ 's and  $U(\gamma(\mathbf{p}'))$ 's are equal to  $\Omega_\beta(\mathbf{p}^*)$  and  $U^*$  for all  $\mathbf{p}' \in \mathcal{P}^{D^*}$ , it follows from (25) that

$$\bar{U}_\beta \geq |\mathcal{P}^{D^*}| U^* \Omega_\beta(\mathbf{p}^*), \quad (26)$$

where  $\mathbf{p}^*$  is a global optimal solution to Problem (UM). Note that

$$V_\beta(U) = |\mathcal{P}^{D^*}| \left( U^* - \bar{U}_\beta \right)^2 \Omega_\beta(\mathbf{p}^*) + \sum_{\mathbf{p} \notin \mathcal{P}^{D^*}} \left( U(\gamma(\mathbf{p})) - \bar{U}_\beta \right)^2 \Omega_\beta(\mathbf{p}) \quad (27.1)$$

$$\leq |\mathcal{P}^{D^*}| U^{*2} \left( 1 - |\mathcal{P}^{D^*}| \Omega_\beta(\mathbf{p}^*) \right)^2 \Omega_\beta(\mathbf{p}^*) + (U^* - U_*)^2 \sum_{\mathbf{p}' \notin \mathcal{P}^{D^*}} \Omega_\beta(\mathbf{p}') \quad (27.2)$$

$$= |\mathcal{P}^{D^*}| U^{*2} \left( 1 - |\mathcal{P}^{D^*}| \Omega_\beta(\mathbf{p}^*) \right)^2 \Omega_\beta(\mathbf{p}^*) + (U^* - U_*)^2 \left( 1 - |\mathcal{P}^{D^*}| \Omega_\beta(\mathbf{p}^*) \right) \quad (27.3)$$

$$\leq \underbrace{U^{*2} \left( 1 - |\mathcal{P}^{D^*}| \Omega_\beta(\mathbf{p}^*) \right)^2 + (U^* - U_*)^2 \left( 1 - |\mathcal{P}^{D^*}| \Omega_\beta(\mathbf{p}^*) \right)}_{\tilde{V}_\beta(U)} \quad (27.4)$$

Specifically, inequality (27.1) is due to (26) as well as the fact that the expected value  $\bar{U}_\beta$  satisfies  $U_* < \bar{U}_\beta \leq U^*$ , and inequality (27.4) is due to the fact that  $\Omega_\beta(\mathbf{p}^*) \leq \frac{1}{|\mathcal{P}^{D^*}|}$ . Inqs. (27) show that  $V_\beta(U)$  is upper bounded by  $\tilde{V}_\beta(U)$ . In fact,

$\tilde{V}_\beta(U)$  is a decreasing function of  $\beta$ . This can be seen by noting that  $\Omega_\beta(\mathbf{p}^*)$  monotonically increases with  $\beta$  and  $\tilde{V}_\beta(U)$  is a decreasing function of  $\Omega_\beta(\mathbf{p}^*)$ .

In particular,  $\tilde{V}_0(U)$  is equal to  $U^{*2} \left( 1 + \frac{|\mathcal{P}^{D^*}|}{|\mathcal{P}^{D^*}|} \right)^2 + (U^* - U_*)^2 \left( 1 + \frac{|\mathcal{P}^{D^*}|}{|\mathcal{P}^{D^*}|} \right)$  when  $\beta = 0$  and  $\tilde{V}_\infty(U)$  is equal to 0 when  $\beta \rightarrow \infty$ . Note that the upper bound  $\tilde{V}_\beta(U)$  is tight when  $\beta \rightarrow \infty$ , as  $V_\beta(U)$  itself equals 0 when  $\beta \rightarrow \infty$ .

Due to the decreasing property of  $\tilde{v}_\beta(U)$ , there exists a  $\beta(\delta)$  for any tolerance  $\delta \geq 0$  that satisfies  $\tilde{v}_\beta(U) \leq \delta$ , and hence  $V_\beta(U) \leq \delta$  for all  $\beta \geq \beta(\delta)$ . Moreover,  $\beta(\delta)$  in (23) can be easily calculated from (27). Thus, Theorem 7 follows. ■

Theorems 5, 6, and 7 show that the optimality of the solution obtained at convergence improves with the increase of  $\beta$ . This together with the convergence rate given in Theorems 3 and 4 gives a guideline on appropriately selecting a  $\beta$  that hits the right balance between convergence speed and solution quality.

## V. SIMULATION RESULTS

In this section, the performance of GLAD is investigated through numerical simulations<sup>3</sup>. In particular, we assume the transmission power  $p_i$  can take any continuous value from  $[0, P_i^{\max}]$ .

### A. Effect of $\beta$ on the Performance of GLAD

We first observe the effect of  $\beta$  on the performance of GLAD. Consider an eight-link network with the channel gain matrix  $\mathbf{G}$ . For such a network, we run GLAD with different  $\beta$ . The attained system utility versus the number of iterations is plotted in Figs. 2 and 3. In particular, the proportional fairness utility

$U(\boldsymbol{\gamma}(\mathbf{p})) = \prod_{i=1}^M \gamma_i(\mathbf{p})$  is considered in Fig. 2 and the total throughput utility

$U(\boldsymbol{\gamma}(\mathbf{p})) = \sum_{i=1}^M \log_2(1 + \gamma_i(\mathbf{p}))$  is considered in Fig. 3. Suppose that  $P_i^{\max} = 1.0$  mW

and  $n_i = 0.1 \mu$  W for each link  $i$ . For comparison purpose, the optimal system utility obtained by the MAPEL algorithm in [11] is also plotted.

$$\mathbf{G} = \begin{bmatrix} 0.1116 & 0.0001 & 0.0040 & 0.0634 & 0.0004 & 0.0004 & 0.0012 & 0.0001 \\ 0.0001 & 0.4939 & 0.0004 & 0.0002 & 0.0411 & 0.0064 & 0.0046 & 0.0024 \\ 0.0004 & 0.0003 & 0.1586 & 0.0039 & 0.0015 & 0.0043 & 0.0006 & 0.0013 \\ 0.0185 & 0.0001 & 0.0159 & 0.7325 & 0.0006 & 0.0007 & 0.0013 & 0.0002 \\ 0.0001 & 0.0359 & 0.0011 & 0.0003 & 0.2913 & 0.1818 & 0.0024 & 0.0316 \\ 0.0001 & 0.0127 & 0.0010 & 0.0002 & 0.0321 & 0.1142 & 0.0010 & 0.4109 \\ 0.0002 & 0.0056 & 0.0007 & 0.0003 & 0.0206 & 0.0034 & 0.1887 & 0.0007 \\ 0.0001 & 0.0040 & 0.0003 & 0.0001 & 0.0021 & 0.0037 & 0.0003 & 0.1041 \end{bmatrix}.$$

<sup>3</sup>In this paper, the algorithms are implemented in MATLAB 7.0, and the time evaluation is based

on a HP Compaq dx7300 desktop with 3.6GHz processors and 1Gb of RAM.

From both figures, it can be seen that the average system utility when the algorithm converges improves with the increase of  $\beta$ . Moreover, the fluctuation (variance) in the system utility decreases as  $\beta$  increases. This is because when  $\beta$  is small, links tend to explore power allocations other than the optimal one from time to time.

In Fig. 4, the mean and the variance of the system utility achieved when the algorithm converges are plotted against  $\beta$ . The total throughput utility is adopted. Again, it can be seen that the mean in the achieved system utility increases with the increase of  $\beta$ . Specifically, the global optimal (maximum) system utility is achieved when  $\beta \rightarrow \infty$ . On the other hand, we can see that the variance (i.e., fluctuation) in the achieved system utility generally follows a decreasing trend and approaches 0 when  $\beta$  is very large. The observations here are consistent with Theorem 6 and Theorem 7, respectively.

The above figures suggest that a large  $\beta$  is always preferable when it comes to the quality of solution obtained at convergence. However, a close observation of Fig. 3 shows that a larger  $\beta$  may lead to slower convergence. This is because the total throughput utility is non-concave in  $\mathbf{p}$  and cannot be convexified through transformation. Thus, there exists more than one local optimal solution. Too large a  $\beta$  may cause the GLAD algorithm to be too greedy, and consequently stuck in a local optimal solution for a long time before exploring other less greedy solutions. Note that such a phenomenon is not observed in Fig. 2. This is because proportional fairness utility maximization problem can essentially be convexified through transformation [3]. Hence, there is only one optimal solution, which is the global optimal one, and the algorithm will not be stuck anywhere even if  $\beta$  is large.

### *B. Complexity Comparison with MAPEL*

In this subsection, we show that GLAD exhibits a faster convergence than its centralized counterpart MAPEL proposed in our earlier work [11]. Consider a six-link network, where the links are randomly placed in a 10m-by-10m area. Other system parameters are the same as those in the above figures. Fig. 5 shows that GLAD converges to the optimal solution in around 50 iterations (i.e., 10.34 seconds), while it takes MAPEL about 700 iterations (i.e., 210.8 seconds) to converge. As such, GLAD can efficiently handle a network size that is considered to be too large for the MAPEL

algorithm.

Before leaving this subsection, we would like to emphasize that MAPEL can only handle system utilities that are monotonic in SINR. Meanwhile, no such requirement is needed in GLAD.

### *C. Benchmark for Existing Distributed Algorithms*

The global optimal power allocation obtained by GLAD can be used as useful benchmark to evaluate the performance of other representative distributed algorithms. In Fig. 6, we compare the average performance of one representative algorithm, namely Asynchronous Distributed Pricing (ADP) in [9] with GLAD under different network densities. Here, the total throughput utility is considered. Other system parameters are the same as in the above figures. We vary the total number of links  $M$  from 10 to 24 and the links are randomly located in a 30m by 30m area. Each point is obtained by averaging over 100 different topologies of the same link density. It can be seen that on average the ADP algorithm has 2 bits/Hz performance degradation compared with GLAD. Percentage wise, the average performance of ADP is quite close to the global optimal one, especially when the number of links is large. Note that this has not been observed before this work, as the global optimal solution was not known before (It is impractical for MAPEL to obtain the global optimal solution when there are many links in the network due to the long computational time). We would like to emphasize that ADP, like most other existing algorithms, only applies when the system utility function is additive, increasing, differentiable, and strictly concave in SINR. In contrast, there is no restriction on the form of system utility in GLAD.

## VI. CONCLUSION

In this paper, we have proposed a distributed power control algorithm, GLAD, that efficiently converges to the set of global optimal solutions despite the non-convexity of power control problems. One key strength of the algorithm is that it applies to all forms of utility functions regardless of the concavity, continuity, differentiability, monotonicity, and whether it is additive across links. Moreover, it exhibits noticeably faster convergence than its centralized counterpart MAPEL. On the other hand, we have analyzed how a control parameter  $\beta$  affects the algorithm performance. This helps to provide a theoretical guideline on how to set a value for  $\beta$  that hits the right

balance between solution quality and convergence speed.

Throughout this paper, we have assumed that the message passing among links is complete, timely and lossless. In practice, however, message passing may subject to delay and losses. Our preliminary work shows that GLAD algorithm is robust against imperfect message passing. This will be investigated in detail in our future work.

APPENDIX A  
PROOF OF THEOREM 3

*Proof:* Let  $\mathbf{Q} = [Q(\mathbf{p}_1, \mathbf{p}_2), \forall \mathbf{p}_1, \mathbf{p}_2 \in \mathcal{P}^D] = \prod_{i=1}^M \mathbf{\Pi}_i$  be the transition matrix

corresponding to one round of transmission power update. Note that  $\mathbf{\Omega}_\beta^{(k)} = \mathbf{V}\mathbf{Q}^k$  and  $\mathbf{\Omega}_\beta = \mathbf{V}\mathbf{Q}^\infty$ , where  $\mathbf{V} = (V(\mathbf{p}), \forall \mathbf{p} \in \mathcal{P}^D)$  is an initial probability distribution on the feasible transmission power set  $\mathcal{P}^D$  and  $\mathbf{Q}^\infty$  is the limit of  $\mathbf{Q}^k$  as  $k \rightarrow \infty$ . Note that every entry  $V(\mathbf{p}) \geq 0$  and  $\sum_{\mathbf{p} \in \mathcal{P}^D} V(\mathbf{p}) = 1$ . Thus,  $\|\mathbf{V}\|_{\text{var}} = \frac{1}{2} \sum_{\mathbf{p} \in \mathcal{P}^D} |V(\mathbf{p})| = \frac{1}{2}$ .

Consequently,

$$\begin{aligned} \|\mathbf{\Omega}_\beta^{(k)} - \mathbf{\Omega}_\beta\|_{\text{var}} &= \|\mathbf{V}\mathbf{Q}^k - \mathbf{V}\mathbf{Q}^\infty\|_{\text{var}} \\ &\leq \|\mathbf{V}\|_{\text{var}} \cdot \|\mathbf{Q}^k - \mathbf{Q}^\infty\|_{\text{var}} \\ &= \frac{1}{2} \|\mathbf{Q}^k - \mathbf{Q}^\infty\|_{\text{var}} \end{aligned} \quad (28)$$

Therefore, to prove Theorem 3, we only need to investigate the property of  $\|\mathbf{Q}^k - \mathbf{Q}^\infty\|_{\text{var}}$ .

According to the theory of Jordan matrix decomposition [18], the square matrix  $\mathbf{Q}$  can be decomposed into

$$\mathbf{Q} = \mathbf{S}\mathbf{J}\mathbf{S}^{-1}, \quad (29)$$

where  $\mathbf{J} = \text{diag}\{\mathbf{J}_1, \mathbf{J}_2, \dots, \mathbf{J}_l\}$  and  $\mathbf{S} = [\mathbf{S}_1, \mathbf{S}_2, \dots, \mathbf{S}_l]$  with  $l \leq |\mathcal{P}^D|$ . Let  $\lambda_{j\beta}$  denote the eigenvalue of matrix  $\mathbf{Q}$ . Assuming that the algebraic multiplicity of eigenvalue  $\lambda_{j\beta}$  is equal to  $m_j$ , matrix  $\mathbf{J}_j$  is a  $m_j \times m_j$  matrix with the following shape

$$\mathbf{J}_j = \begin{pmatrix} \lambda_{j\beta} & 1 & & 0 \\ & \lambda_{j\beta} & \ddots & \\ & & \ddots & 1 \\ 0 & & & \lambda_{j\beta} \end{pmatrix} = \lambda_{j\beta} \cdot \mathbf{I}_{m_j} + \underbrace{\begin{pmatrix} 0 & 1 & & 0 \\ & 0 & \ddots & \\ & & \ddots & 1 \\ 0 & & & 0 \end{pmatrix}}_{\mathbf{E}_j}, \quad (30)$$

where matrices  $\mathbf{I}_{m_j}$  and  $\mathbf{E}_j$  are an identity matrix and a nilpotent matrix<sup>4</sup>, respectively. Matrix  $\mathbf{S}_j$  is a  $|\mathcal{P}^D| \times m_j$  matrix such that its  $n$ th column vector  $\mathbf{s}_{j,n}$  satisfies  $(\mathbf{Q} - \lambda_{j\beta} \mathbf{I}_{|\mathcal{P}^D|})^n \mathbf{s}_{j,n} = 0$ , where matrix  $\mathbf{I}_{|\mathcal{P}^D|}$  is an identity matrix.

Perron-Frobenius theorem [18] says that, for a positive matrix, there exists a unique largest eigenvalue  $\rho$  such that any other eigenvalue is strictly smaller than  $\rho$  in absolute value. Meanwhile only eigenvalue  $\rho$  is associated with a positive eigenvector. Note that  $\mathbf{Q}$  is a positive matrix and has a positive eigenvector  $\mathbf{\Omega}_\beta$  satisfying  $\mathbf{\Omega}_\beta \mathbf{Q} = \mathbf{\Omega}_\beta$ . Therefore, the largest eigenvalue of matrix  $\mathbf{Q}$  is 1 and any other eigenvalue is strictly smaller than 1 in absolute value. With loss of generality, let  $\lambda_{1\beta} = 1 > |\lambda_{2\beta}| \geq \dots \geq |\lambda_{l\beta}|$ . Then,  $\mathbf{J}_1 = [1]$  and  $\mathbf{S}_1$  is a  $|\mathcal{P}^D| \times 1$  matrix, as there is only one largest eigenvalue for matrix  $\mathbf{Q}$ .

Taking the  $k$ th power of  $\mathbf{Q}$ , we have

$$\mathbf{Q}^k = \mathbf{S} \begin{pmatrix} 1 & 0 & & 0 \\ 0 & \mathbf{J}_2^k & & \\ & & \ddots & \\ 0 & & & \mathbf{J}_l^k \end{pmatrix} \mathbf{S}^{-1} \xrightarrow{k \rightarrow \infty} \mathbf{Q}^\infty = \mathbf{S} \underbrace{\begin{pmatrix} 1 & 0 & & 0 \\ 0 & 0 & & \\ & & \ddots & \\ 0 & & & 0 \end{pmatrix}}_{\mathbf{Z}} \mathbf{S}^{-1}. \quad (31)$$

Since matrix  $\mathbf{E}_j$  is nilpotent and  $|\lambda_{j\beta}| < 1$ , we get

$$\begin{aligned} \mathbf{J}_j^k &= [\lambda_{j\beta} \cdot \mathbf{I}_{m_j} + \mathbf{E}_j]^k = \lambda_{j\beta}^k \cdot \mathbf{I}_{m_j} + k \lambda_{j\beta}^{k-1} \cdot \mathbf{E}_j + \dots + k \lambda_{j\beta} \cdot \mathbf{E}_j^{k-1} + \mathbf{E}_j^k \\ &= \lambda_{j\beta}^k \cdot \mathbf{I}_{m_j} + \frac{k \lambda_{j\beta}^k}{\lambda_{j\beta}} \cdot \mathbf{E}_j + \dots + \frac{k! \lambda_{j\beta}^k}{(m_j - 1)!(k - m_j + 1)! \lambda_{j\beta}^{m_j - 1}} \cdot \mathbf{E}_j^{m_j - 1} \\ &\leq C_\beta \lambda_{j\beta}^k [\mathbf{I}_{m_j} + \mathbf{E}_j + \dots + \mathbf{E}_j^{m_j - 1}] \end{aligned} \quad (32)$$

for  $C_\beta > 0$ . This implies that any  $\mathbf{J}_j^k$  satisfies

$$\mathbf{J}_j^k \leq C_\beta \lambda_{2\beta}^k [\mathbf{I}_{m_j} + \mathbf{E}_j + \dots + \mathbf{E}_j^{m_j - 1}]. \quad (33)$$

due to the fact that  $|\lambda_{2\beta}| \geq \dots \geq |\lambda_{l\beta}|$ . Therefore,

<sup>4</sup>The non-negative square matrix  $\mathbf{E}_j$  is defined to be nilpotent, since there exists an integer  $m_j > 0$  such that  $\mathbf{E}_j^{m_j} = 0$ .

$$\begin{aligned}
\|\mathbf{Q}^k - \mathbf{Q}^\infty\|_{\text{var}} &\leq \|\mathbf{S}\|_{\text{var}} \cdot \|\mathbf{J}^k - \mathbf{Z}\|_{\text{var}} \cdot \|\mathbf{S}^{-1}\|_{\text{var}} \\
&\leq \|\mathbf{I}_{|\mathcal{P}^D|}\|_{\text{var}} \cdot \|\mathbf{J}^k - \mathbf{Z}\|_{\text{var}} \\
&\leq \underbrace{\frac{1}{4} C_\beta |\mathcal{P}^D| \sum_{j=2}^L \frac{m_j(m_j+1)}{2}}_{c_\beta} |\lambda_{2\beta}|^k.
\end{aligned} \tag{34}$$

It is clear that  $c_\beta$  is determined by  $\mathbf{Q}$ , because every  $m_j$  is equal to the algebraic multiplicity of eigenvalue  $\lambda_{j\beta}$  of matrix  $\mathbf{Q}$ . Correspondingly, together with (33), it follows that

$$\|\boldsymbol{\Omega}_\beta^{(k)} - \boldsymbol{\Omega}_\beta\|_{\text{var}} \leq c_\beta |\lambda_{2\beta}|^k. \tag{35}$$

Therefore, Theorem 3 follows. ■

#### REFERENCES

- [1] M. Chiang, P. Hande, T. Lan, and C. W. Tan, "Power control in wireless cellular networks," in *Foundations and Trends in Networking*, vol. 2, no. 4, pp. 381-533, Jul. 2008.
- [2] D. Julian, M. Chiang, D. O. Neill, and S. Boyd, "Qos and fairness constrained convex optimization of resource allocation for wireless cellular and ad hoc networks," *Proc. IEEE INFOCOM*, vol. 2, pp. 477-486, Jun. 2002.
- [3] M. Chiang, C. W. Tan, D. Palomar, D. O. Neill, and D. Julian, "Power control by geometric programming," *IEEE Trans. Wireless Commun.*, vol. 1, no. 7, pp. 2640-2651, Jul. 2007.
- [4] C. U. Saraydar, N. B. Mandayam, and D. J. Goodman, "Efficient power control via pricing in wireless data networks," *IEEE Trans. Commun.*, vol. 50, no. 2, pp. 291-303, Feb. 2002.
- [5] T. Alpcan, T. Basar, R. Srikant, and E. Altman, "CDMA uplink power control as a noncooperative game," *Wireless Networks*, vol. 8, pp. 659-670, 2002.
- [6] M. Rasti, A. R. Sharafat, and B. Seyfe, "Pareto-efficient and goal-driven power control in wireless networks: a game-theoretic approach with a novel pricing scheme," *IEEE/ACM Trans. on Networking*, vol. 17, no. 2, pp. 556-569, Apr., 2009.
- [7] S. Sharma and D. Teneketzis, "An externalities-based decentralized optimal power allocation algorithm for wireless networks," *IEEE/ACM Trans. on Networking*, vol. 17, no. 6, pp. 1819-1831, Dec. 2009.

- [8] P. Hande, S. Rangan, M. Chiang, and X. Wu, "Distributed uplink power control for optimal SIR assignment in cellular data networks," *IEEE/ACM Trans. Networking*, vol. 16, no. 6, pp. 1420-1433, Dec. 2008.
- [9] J. Huang, R. Berry, and M. Honig, "Distributed interference compensation for wireless networks," *IEEE J. Select. Areas Commun.*, vol. 24, no. 5, May 2006.
- [10] Z. Q. Luo and S. Zhang, "Dynamic spectrum management: complexity and duality," *IEEE Journal of Selected Topics in Signal Processing*, vol. 2, no. 1, pp. 57-73, Feb. 2008.
- [11] L. P. Qian, Y. J. Zhang, and J. W. Huang, "MAPEL: achieving global optimality for a non-convex wireless power control problem," *IEEE Trans. Wireless Commun.*, vol. 8, no. 3, pp. 1553-1563, Mar. 2009.
- [12] H. R. Varian, "Intermediate microeconomics: a modern approach," *Chapter 4*, Norton, New York, 1999.
- [13] S. Geman and D. Geman, "Stochastic relaxation, gibbs distributions, and the bayesian restoration of images," *IEEE Trans Pattern Anal Machine Intelligence*, vol. 6, no. 6, pp. 721-741, 1984.
- [14] G. Winkler, "Image Analysis, random fields and markov chain monte carlo methods: a mathematical introduction," 2nd ed., Springer Verlag, 2003.
- [15] P. Salamon, P. Sibani, and R. Frost, "Facts, conjectures, and improvements for simulated annealing," SIAM Monographs, 2002.
- [16] J. S. Rosenthal, "Rate of convergence for gibbs sampling for variance component models," *Ann. Statist.* 23, vol. b, pp. 740-761, 1995.
- [17] R. Chen, J. S. Liu, and X. Wang, "Convergence analysis and comparisons of markov chain monte carlo algorithms in digital communications," *IEEE Trans. Signal Processing*, vol. 20, no. 2, Feb. 2002.
- [18] A. Berman and R. J. Plemmons, "Nonnegative martices in the mathematical sciences," Philadelphia, PA: SIAM, 1994.

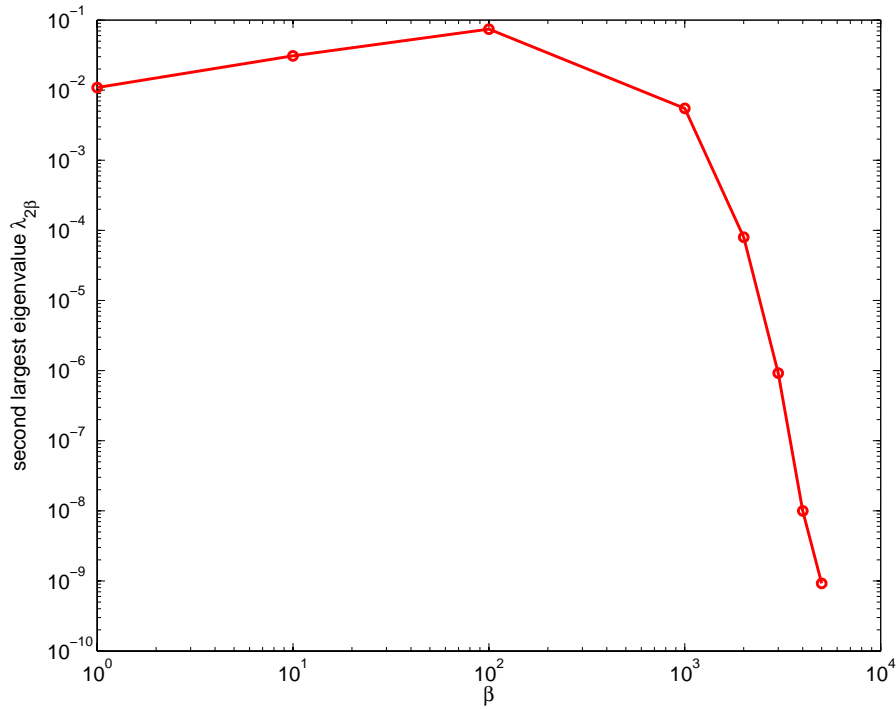


**Fig. 1.** The second largest eigenvalue  $\lambda_{2\beta}$  for different  $\beta$ . Here, the total throughput utility is adopted for a 4-link network.

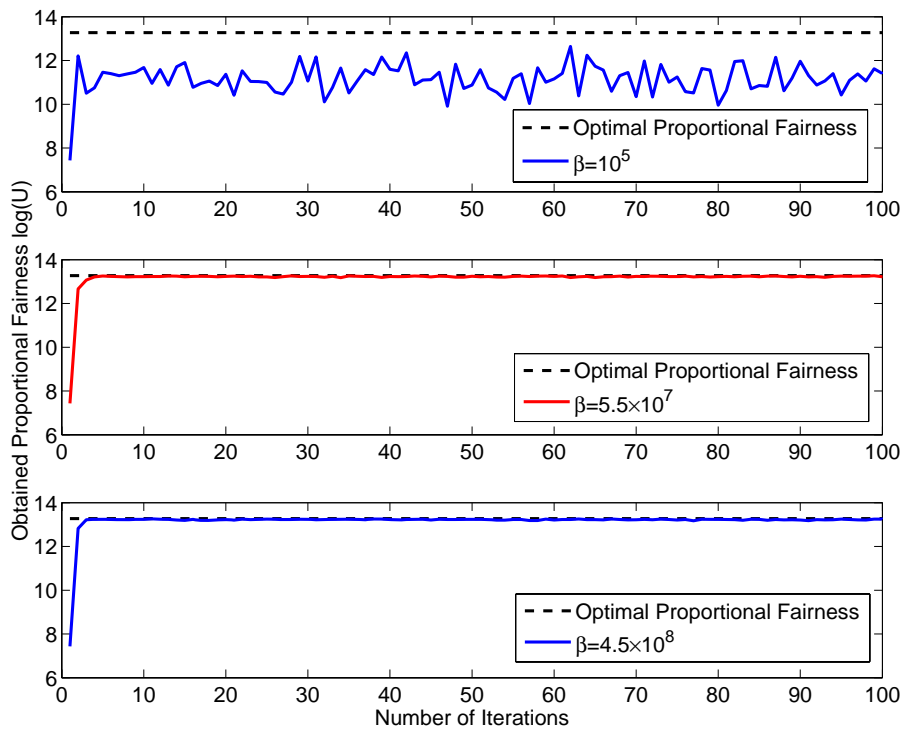


**Fig. 2.** Obtained Proportional Fairness and number of iterations for different  $\beta$ .

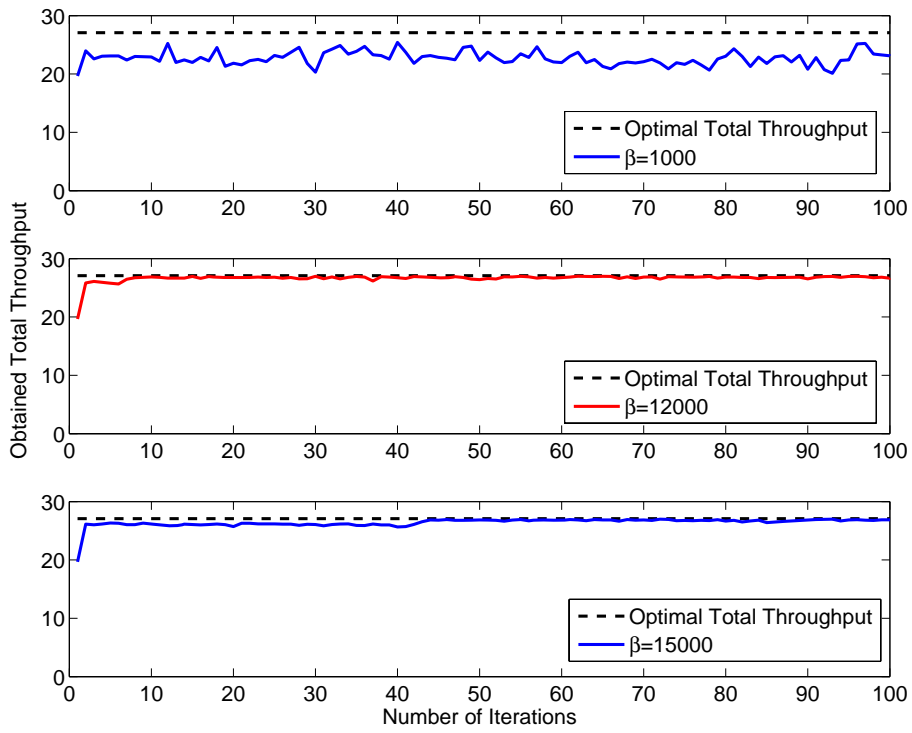


Fig. 3. Obtained Total Throughput and number of iterations for different  $\beta$ .

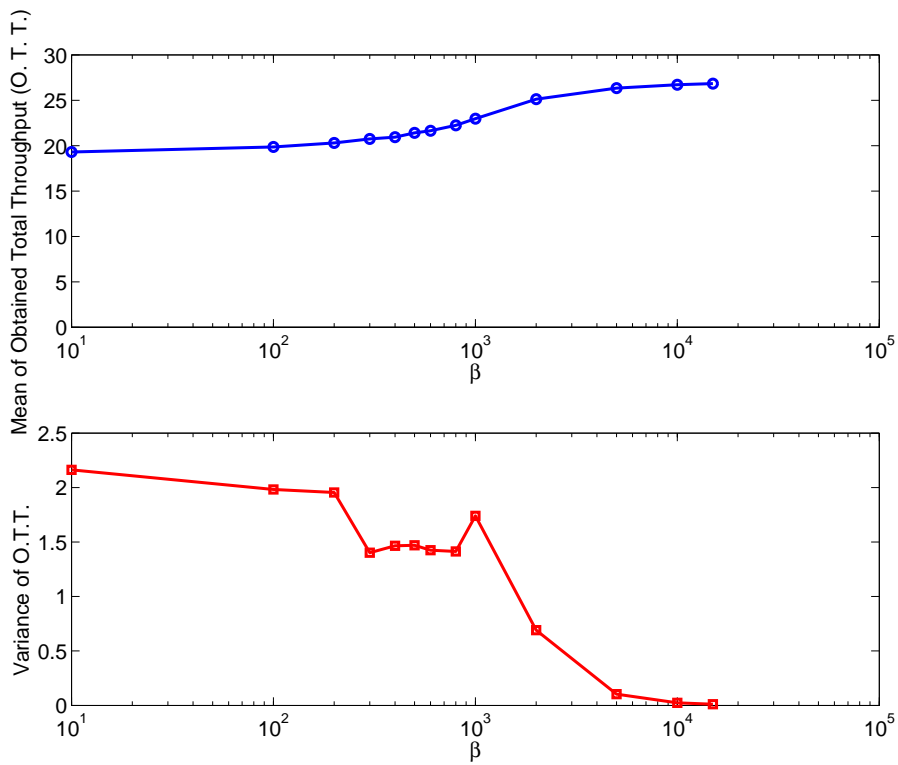


Fig. 4. The mean and the variance in the achieved system utility for different  $\beta$ .

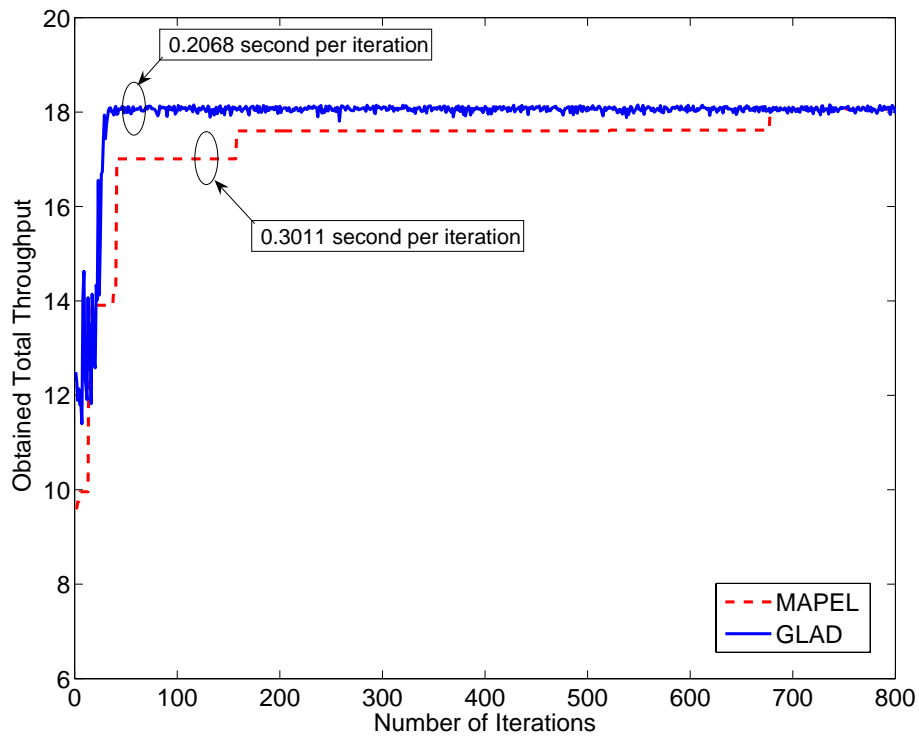


Fig. 5. The complexity comparison between GLAD and MAPEL.

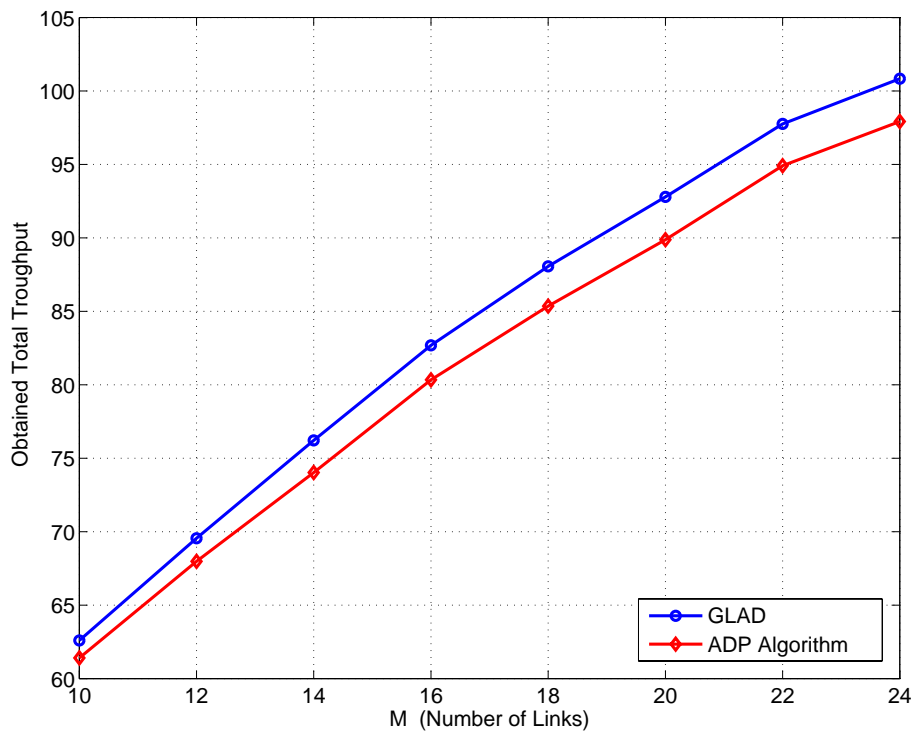


Fig. 6. Average total throughput of different algorithms in  $M$ -link networks.